

## Coupling between the transverse and longitudinal components of an electron in resonant tunneling

Xue-Hua Wang, Ben-Yuan Gu, and Guo-Zhen Yang  
 CCAST (World Laboratory) P.O. Box 8730, Beijing 100080, China  
 and Institute of Physics, Academia, P.O. Box 603, Beijing 100080, China\*  
 (Received 29 May 1996; revised manuscript received 28 October 1996)

In this paper we present formulas for the transmission coefficient in multibarrier heterostructures when taking into account the space-dependent electron effective mass and the coupling between components of the motion of an electron in directions parallel and perpendicular to the interfaces. We find that the coupling leads to a decrease of the effective barrier height seen by the electron. The numerical calculations are carried out for the double- and triple-barrier heterostructures consisting of GaAs/Ga<sub>1-x</sub>Al<sub>x</sub>As. Our results show that the coupling effect leads not only significantly to a shift of resonant peaks toward the low-energy region, but also causes the broadening of resonant peaks and the reduction of the peak-to-valley ratio in the transmission spectrum. The coupling becomes more pronounced for higher-lying resonant states. In addition, the variation of the coupling strength with the concentration  $x$  of Al is also investigated. [S0163-1829(97)08315-X]

Since the pioneering work of Tsu and Esaki<sup>1,2</sup> on the resonant-tunneling problem in semiconductor heterostructures, the relevant subject has attracted a great deal of attention owing to the advance in microfabrication technique and potential applications to electronic devices. There mainly exist two theoretical frameworks for dealing with resonant-tunneling problems. One is the tight-binding model (TBM).<sup>3-5</sup> The other is the parabolic-band effective-mass approximation (PBEMA). In the PBEMA, the coherent tunneling model (CTM) (Refs. 6-8) and the sequential tunneling model (STM) (Refs. 9-12) have been proposed and developed for investigating resonant-tunneling characteristics in multibarrier heterostructures. In the CTM, an electron keeps its phase memory in the tunneling process, which is regarded as a coherent transmission process and described by the eigenstate of the electron in the total structure. In the STM, the electron loses its phase memory in the tunneling process, which is regarded as a series of successive transition processes with phase incoherence. The CTM and STM in the PBEMA are restricted to the assumption that the components of the motion of the electron in the directions parallel (transverse) and perpendicular (longitudinal) to the interfaces are decoupled. However, this assumption is incorrect when the difference of the effective mass of the electron in the barrier and well materials is taken into account. It arises for the following reason. The conservation of the transverse momentum of the electron results in a breakdown of the conservation for the transverse kinetic energy of the electron when considering the space dependence of the electron effective mass. As a result, a coupling between the longitudinal and transverse components of the motion of the electron emerges for structures with a position-dependent electron effective mass. The introduction of the coupling term is a mathematical price we have to pay, while the variable separation approach is used in solving the Schrödinger equation to treat a three-dimensional (3D) problem with a 1D equation. The coupling leads to a significant dependence of the effective barrier height "seen" by the electron on the transverse momentum of the electron. Thus the longitudinal part  $\Phi(z)$  of the electron wave function depends substantially on the transverse momentum of the electron, when there exists a

large difference of the effective mass of the electron in the barrier and well materials. Recently, in the framework of the TBM, Boykin studied the effect of the transverse wave vector on the resonant tunneling in double-barrier heterostructures consisting of InAs/AlSb.<sup>13</sup> In the framework of the PBEMA, Paranjape calculated the dependence of the tunneling time and transmission coefficient on the incident angle for an electron tunneling through a single-barrier heterostructure.<sup>14</sup> These studies showed that the influence of the transverse component of motion of the electron on the longitudinal transport process is significant.

The aim of this work is to explore the effect of coupling between the transverse motion and the longitudinal motion of the electron on resonant-tunneling characteristics in multibarrier heterostructures based upon the CTM in the PBEMA. First, we present the form of an effective barrier height as a function of the transverse wave number of the electron for the electron-tunneling process in structures with a space-dependent electron effective mass. Second, we derive the relevant formula for the transmission probability depending on both the transverse wave number and the longitudinal kinetic energy of an incident electron. Finally, we present numerical results for the double- and triple-barrier heterostructures consisting of GaAs/Ga<sub>1-x</sub>Al<sub>x</sub>As and give a brief conclusion.

In the framework of the PBEMA, the Hamiltonian of an electron in the multibarrier heterostructures is

$$\hat{H} = \frac{1}{2m(z)} \hat{p}_{xy}^2 + \frac{1}{2} \hat{p}_z \frac{1}{m(z)} \hat{p}_z + U(z), \quad (1)$$

where the  $z$  axis represents the growth direction of heterostructures,  $\hat{p}_{xy}$  and  $\hat{p}_z$  denote the electron momentum operators parallel and perpendicular to the interface, respectively,  $U(z)$  is the potential-energy function, and  $m(z)$  is the space-dependent electron effective mass.  $U(z)$  and  $m(z)$  are, respectively, defined as follows:

$$U(z) = \begin{cases} 0 & (\text{in the well}) \\ U_0 & (\text{in the barrier}), \end{cases} \quad (2)$$

$$m(z) = \begin{cases} m_w^* & (\text{in the well}) \\ m_b^* & (\text{in the barrier}), \end{cases} \quad (3)$$

where  $U_0$  is the offset of the conduction-band edge between the well and the barrier, and  $m_w^*$  and  $m_b^*$  are the electron effective masses for the conduction-band edge in the well and the barrier regions, respectively. Therefore, the form of the Schrödinger equation governing the electron motion in the well and the barrier regions can be written, respectively, as

$$-\hbar^2/2m_w^* \nabla^2 \Psi = E \Psi \quad (\text{in the well}), \quad (4)$$

$$-(\hbar^2/2m_b^*) \nabla^2 \Psi + U_0 \Psi = E \Psi \quad (\text{in the barrier}),$$

where  $E$  is the total energy of an electron. Because  $[\hat{p}_{xy}, \hat{H}] = 0$ , the transverse momentum  $\mathbf{p}_{xy} = (p_x, p_y)$  of the electron preserves conservation in the tunneling process. Hence the wave function of the electron should be of the form

$$\Psi = \exp(i\mathbf{k}_{xy} \cdot \mathbf{r}) \Phi(z), \quad (5)$$

where  $\mathbf{k}_{xy} = (p_x/\hbar, p_y/\hbar)$  and  $\mathbf{r} = (x, y)$ , respectively, are the transverse wave vector and the transverse coordinate of the electron in the plane parallel to the interface.  $\Phi(z)$  satisfies the 1D Schrödinger equation

$$-\frac{\hbar^2}{2m_w^*} \frac{d^2 \Phi(z)}{dz^2} = E_z^w \Phi(z) \quad (\text{in the well}), \quad (6)$$

$$-\frac{\hbar^2}{2m_b^*} \frac{d^2 \Phi(z)}{dz^2} + U_0 \Phi(z) = E_z^b \Phi(z) \quad (\text{in the barrier}),$$

where  $E_z^w = E - E_{zy}^w$  and  $E_z^b = E - E_{zy}^b$  are the longitudinal energies of the electron in the well and barrier, respectively. Here  $E_{xy}^w = \hbar^2 k_{xy}^2 / 2m_w^*$  and  $E_{xy}^b = \hbar^2 k_{xy}^2 / 2m_b^*$  are, respectively, the transverse kinetic energy of the electron in the well and the barrier. Thus it can be seen that both the transverse kinetic-energy and longitudinal energy components of the electron no longer keep their conservation individually when taking into account the difference of effective mass of the electron in the well and barrier materials. We introduce an effective barrier height  $U(k_{xy})$  for tunneling of electrons along the  $z$  direction as

$$U(k_{xy}) = U_0 - (1 - \gamma) (\hbar^2 k_{xy}^2 / 2m_w^*), \quad (7)$$

where  $\gamma = m_w^* / m_b^*$ . With the use of Eq. (7), Eq. (6) can then be rewritten as

$$-\frac{\hbar^2}{2m_w^*} \frac{d^2 \Phi(z)}{dz^2} = E_z^w \Phi(z) \quad (\text{in the well}), \quad (8)$$

$$-\frac{\hbar^2}{2m_b^*} \frac{d^2 \Phi(z)}{dz^2} + U(k_{xy}) \Phi(z) = E_z^w \Phi(z) \quad (\text{in the barrier}).$$

From Eqs. (7) and (8), it is evident that there exists a coupling between the components of the motion of the electron in directions parallel and perpendicular to the interfaces, as long as the difference of the effective mass of the electron in the well and barrier regions is taken into account, i.e.,  $\gamma \neq 1$ . This coupling can be interpreted as meaning that the effective barrier height “seen” by the electron is no longer a constant  $U_0$ , and that it depends on the transverse wave number of the electron.

We now employ Eq. (8) to calculate the transmission probability of an electron tunneling through  $N$ -barrier heterostructures. Assume that the wave vector of the incident electron is  $\mathbf{k} = (k_{xy}, k_z)$ ; the 1D wave functions in the incident and outgoing regions can be written as follows:

$$\Phi_I(z) = \exp(ik_z z) + r \exp(-ik_z z) \quad (\text{in the incident region}), \quad (9)$$

$$\Phi_T(z) = t \exp(ik_z z) \quad (\text{in the outgoing region}), \quad (10)$$

where  $k_z = (2m_w^* E_z)^{1/2} / \hbar$ , and  $E_z$  is the longitudinal kinetic energy of the incident electron. The wave functions in the  $j$ th barrier and the  $j$ th well regions are written as

$$\Phi_b^j(z) = C_b^j \exp(k_b z) + D_b^j \exp(-k_b z) \quad (\text{in the } j\text{th barrier}), \quad (11)$$

$$\Phi_w^j(z) = C_w^j \exp(ik_z z) + D_w^j \exp(-ik_z z) \quad (\text{in the } j\text{th well}), \quad (12)$$

where  $k_b = \{2m_b^* [U(k_{xy}) - E_z]\}^{1/2} / \hbar$ .

Current flux density conservation requires the continuity for both  $\Phi(z)$  and  $\Phi'(z)/m(z)$  at each interface. This leads to relationships between the coefficients  $r$  and  $t$ :

$$\begin{pmatrix} 1 \\ r \end{pmatrix} = \frac{1}{2} \begin{pmatrix} 1 & -ik_z^{-1} \\ 1 & ik_z^{-1} \end{pmatrix} \hat{M} \begin{pmatrix} 1 & 1 \\ ik_z & -ik_z \end{pmatrix} \begin{pmatrix} t \\ 0 \end{pmatrix}, \quad (13)$$

where  $\hat{M}$  is the global transfer matrix with  $2 \times 2$  dimensions, and it can be expressed as the cascading of a series of the individual barrier and well transfer matrices in sequence,

$$\hat{M} = \left[ \prod_{j=1}^{N-1} \hat{M}_b(b_j) \hat{M}_w(a_j) \right] \hat{M}_b(b_N), \quad (14)$$

where  $b_j$  and  $a_j$  are the widths of the  $j$ th barrier and  $j$ th well, respectively;  $\hat{M}_b(b_j)$  and  $\hat{M}_w(a_j)$  correspond to the transfer matrices for the  $j$ th barrier and  $j$ th well, respectively:

$$\hat{M}_b(b_j) = \begin{pmatrix} \cosh(k_b b_j) & -(\gamma k_b)^{-1} \sinh(k_b b_j) \\ -\gamma k_b \sinh(k_b b_j) & \cosh(k_b b_j) \end{pmatrix}, \quad (15)$$

$$\hat{M}_w(a_j) = \begin{pmatrix} \cos(k_z a_j) & -(k_z)^{-1} \sin(k_z a_j) \\ k_z \sin(k_z a_j) & \cosh(k_z a_j) \end{pmatrix}. \quad (16)$$

From Eq. (13), it is readily found that the transmission amplitude  $t$  is determined by

$$t = \frac{2}{M_{11} + M_{22} + i(k_z M_{12} - k_z^{-1} M_{21})}, \quad (17)$$

where  $M_{ij}$  is the elements of the global transfer matrix. Finally, the transmission probability  $T$  is given by

$$T(k_{xy}, E_z) = t^* t. \quad (18)$$

It is evident from these expressions that the transmission probability of an electron tunneling through multibarrier heterostructures depends upon both the transfer wave number and the longitudinal kinetic energy of the incident electron.

To gain a quantitative feeling about the effect of the coupling between the transverse motion and the longitudinal motion of the electron on resonant tunneling, it is necessary to carry out numerical calculations for the specific cases. We consider double- and triple-barrier heterostructures consisting of GaAs/Ga<sub>1-x</sub>Al<sub>x</sub>As, where  $x$  represents the concentration of Al. In this system, the offset of the conduction-band edge and the effective mass of the electron are approximately evaluated by the expressions<sup>15</sup>

$$U_0 = \begin{cases} 0.75x & (\text{eV}) & (0 < x \leq 0.45) \\ 0.75x + 0.69(x - 0.45)^2 & (\text{eV}) & (0.45 \leq x \leq 1) \end{cases} \quad (19)$$

and

$$\begin{cases} m_b^* = (0.067 + 0.083x)m_e & (0 < x \leq 1) \\ m_w^* = 0.067m_e, \end{cases} \quad (20)$$

where  $m_e$  is the free-electron mass. In the following calculations, the value of  $m_e$  is taken by  $9.1094 \times 10^{-31}$  (Kg).

The dependence of the transmission probability  $T$  on the longitudinal kinetic energy and the transverse wave number of the electron is shown in Figs. 1(a) and 1(b) for the double-barrier heterostructures with an Al concentration of  $x = 0.45$  (yielding an offset of the conduction-band edge to be  $U_0 = 337.5$  meV), a barrier width of  $b_1 = b_2 = 65$  Å, and a well width of  $a_1 = 50$  Å. From the three-dimensional plot in Fig. 1(a),  $\log_{10}(T) - (E_z, k_{xy})$ , it can be found that two sharp peaks shift toward the low-energy region with the increase of the transverse wave number  $k_{xy}$ . Moreover, the shift of the second peak is much greater than that of the first peak. This shift can be more clearly observed from the two-dimensional plot in Fig. 1(b),  $\log_{10}(T) - E_z$ , for four different values of  $k_{xy}$ . Curves  $a-d$  correspond to different  $k_{xy} = 0.00, 0.02, 0.04,$  and  $0.06$  Å<sup>-1</sup>, respectively. The relative shifts of the resonant peak position in curves  $b, c,$  and  $d$  are  $-1, -4,$  and  $-8$  meV for the first resonant peak, and  $-4, -17,$  and  $-42$  meV for the second resonant peak, comparing with the corresponding resonant peak positions in curves  $a$  with  $k_{xy} = 0$ . In addition, it is also seen that with an increase of  $k_{xy}$  the width of resonant peaks broadens, and the peak-to-valley ratio in the transmission spectrum reduces. It is evident that the

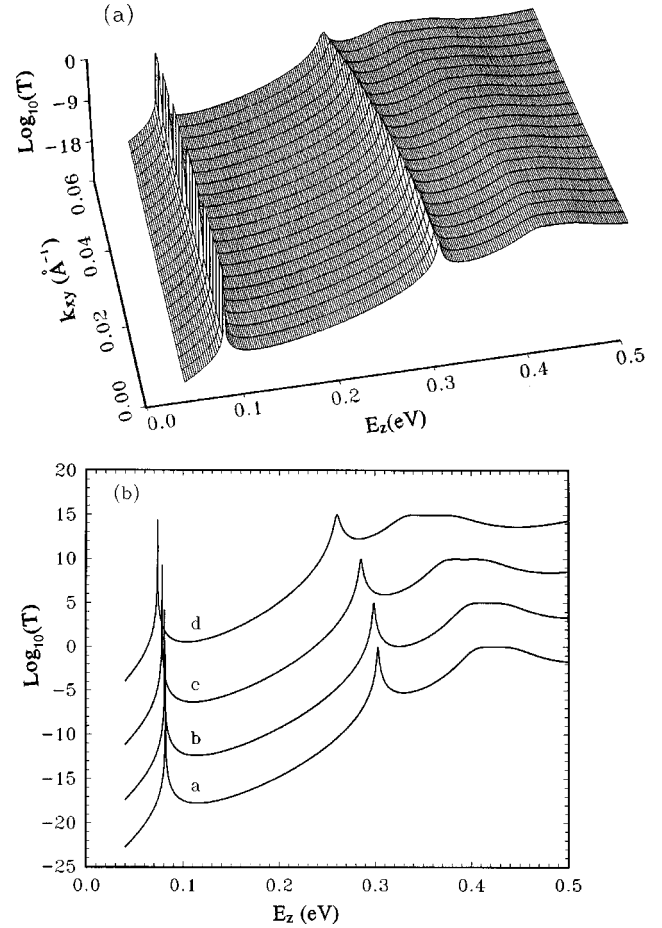


FIG. 1. Base-10 logarithm of the transmission probability  $T$  as a function of the longitudinal kinetic energy  $E_z$ , and the transverse wave number  $k_{xy}$  of an incident electron for a symmetric double-barrier heterostructure. The relevant physical and geometric parameters for the system have been addressed in the text. (a) Three-dimensional (3D) plot; (b)  $\log_{10}(T) - E_z$  plot for four different values of  $k_{xy}$ . Curves  $a-d$  correspond to the cases of  $k_{xy} = 0.00, 0.02, 0.04,$  and  $0.06$  Å<sup>-1</sup>, respectively. For clarity, two consecutive curves are vertically offset.

influence of the transverse motion of the electron on higher-lying resonant states for resonant tunneling is more remarkable than on the lower-lying resonant states.

These effects above can also be observed in the triple-barrier heterostructures. The 3D plot of the transmission probability as functions of the transverse wave number and the longitudinal kinetic energy of the incident electron is shown in Fig. 2 for the triple barrier structure with an Al concentration of  $x = 0.45$  (yielding  $U_0 = 337.5$  meV), barrier widths of  $b_1 = b_3 = 65$  Å and  $b_2 = 20$  Å, and a well width of  $a_1 = a_2 = 50$  Å. In this figure, as expected, four sharp resonant peaks emerge, owing to the splitting of original resonant levels generated from the coupling between the quasibound states residing in two adjacent quantum wells. As observed in the double-barrier heterostructures, with the increase of  $k_{xy}$  these resonant peaks move toward the low-energy region, and moreover the shifts of two higher-lying resonant peaks are much larger than that of two lower-lying resonant peaks. In addition, the variations of the resonant peak width and the peak-to-valley ratio with  $k_{xy}$  are the same as that observed in Figs. 1(a) and 1(b).

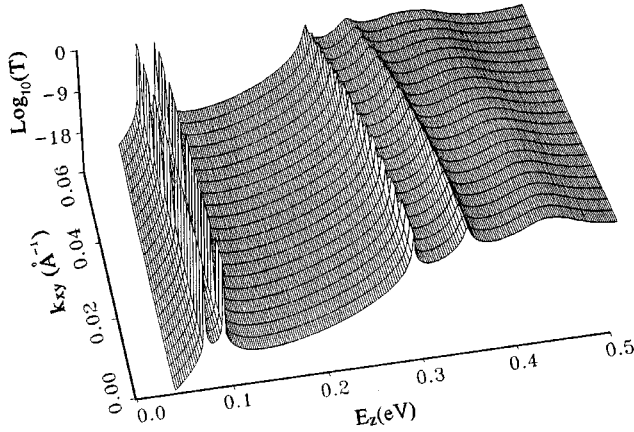


FIG. 2. Three-dimensional (3D) plot of the base-10 logarithm of the transmission probability  $T$  as functions of the longitudinal kinetic energy  $E_z$  and the transverse wave number  $k_{xy}$  of an incident electron for a symmetric triple-barrier heterostructure. The relevant physical and geometric parameters for the system are described in the text.

The physics of all the results above can be easily understood. From the expression of the effective barrier height ‘‘seen’’ by electrons in Eq. (7), it can be seen that the increase of the transverse wave number leads to a decrease of the effective barrier height. Consequently, effects such as the shift of resonant peaks toward the low-energy region, the width broadening of the resonant peaks, and the reduction of the peak-to-valley ratio are natural consequences owing to the decrease of the effective barrier height.

To obtain insight into the influence of different concentration  $x$  of Al on the strength of the coupling between the longitudinal motion and the transverse motion of the electron, the relative shifts of the resonant peak position for the case of  $k_{xy}=0.04 \text{ \AA}^{-1}$  comparing with that of  $k_{xy}=0$  in the double-barrier heterostructure are shown in Fig. 3 as a function of the concentration  $x$  of Al.  $\Delta E_1$  and  $\Delta E_2$  represent, respectively, the magnitudes of the relative shift of resonant peak position for the first and second resonant peaks in the transmission probability spectrum. The solid and dashed lines are for the  $\Delta E_1-x$  and  $\Delta E_2-x$  curves, respectively. It can be seen that  $\Delta E_1$  decreases monotonically with the increase of the concentration  $x$  of Al. However, there exists a maximum in the  $\Delta E_2-x$  curve (dashed line) at  $x \approx 0.37$ . Equations (19) and (20) show that the increase of  $x$  results in both a lift of  $U_0$  and an increase of  $m_b^*$ . From Eq. (7) it can be found that the lift of  $U_0$  leads to an increase of the effec-

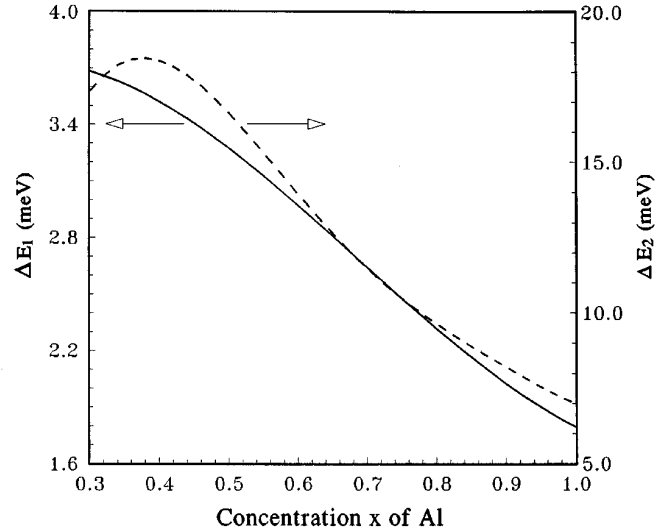


FIG. 3. Magnitude of the relative shift of resonant peak position in tunneling spectrum as a function of the concentration  $x$  of Al in the double-barrier heterostructure with the same structural parameters as Fig. 1 for a given value of  $k_{xy}=0.04 \text{ \AA}^{-1}$ . The shift amount of the peak position is evaluated with respect to the corresponding peak position in the case of  $k_{xy}=0.00 \text{ \AA}^{-1}$ . The solid curve describes the relative shift for the first resonant peak, and the dashed curve the second resonant peak.

tive barrier height, while the increase of  $m_b^*$  plays an opposite role, leading to a decrease of the effective barrier height. In other words, the lift of  $U_0$  should weaken the coupling effect, while the increase of  $m_b^*$  should strengthen this coupling effect. Hence the appearance of the maximum in the  $\Delta E_2-x$  curve is reasonable. The monotonic decrease of  $\Delta E_1$  might be attributed to the fact that the effect of the lift of  $U_0$  is much stronger than the other, and completely dominates the coupling effect for the lower-lying resonant state.

In conclusion, our studies have shown that coupling between components of the motion of the electron in directions parallel and perpendicular to the interfaces can substantially affect resonant-tunneling characteristics in the multibarrier heterostructures. In particular, for higher-lying resonant states this coupling effect becomes more important for obtaining the correct tunneling spectrum.

The authors wish to thank the reviewers for their valuable suggestions and recommendations for revising our manuscript. This study was supported by the National Natural Science Foundation of China.

\*Mailing address. Electronic mail address:  
guby@aphy01.iphy.ac.cn

<sup>1</sup>R. Tsu and L. Esaki, Appl. Phys. Lett. **22**, 562 (1973).

<sup>2</sup>L. L. Chang, L. Esaki, and R. Tsu, Appl. Phys. Lett. **24**, 593 (1974).

<sup>3</sup>K. V. Roussean, K. L. Wang, and J. N. Schulman, Appl. Phys. Lett. **54**, 1341 (1989).

<sup>4</sup>T. B. Boykin, Jan P. A. Van der Wagt, and J. S. Harris, Phys. Rev. B **43**, 4777 (1991).

<sup>5</sup>M. S. Kiledjian, J. N. Schulman, and K. L. Wang, Phys. Rev. B **46**, 16 012 (1992).

<sup>6</sup>M. Y. Azbel, Phys. Rev. B **28**, 4106 (1983).

<sup>7</sup>B. Ricco and M. Y. Azbel, Phys. Rev. B **29**, 1970 (1984).

<sup>8</sup>J. P. Peng, H. Chen, and S. H. Zhou, J. Phys. Condens. Matter **1**, 5451 (1989).

<sup>9</sup>S. Luryi, Appl. Phys. Lett. **47**, 490 (1985).

<sup>10</sup>M. C. Payen, J. Phys. C **19**, 1145 (1986).

<sup>11</sup>T. Weil and B. Vinter, Appl. Phys. Lett. **50**, 1281 (1987).

<sup>12</sup>X. H. Wang, J. P. Peng, T. Z. Li, S. W. Gu, W. S. Li, and Y. Y. Yeung, J. Phys. Condens. Matter **6**, 10031 (1994).

<sup>13</sup>T. B. Boykin, Phys. Rev. B **51**, 4289 (1995).

<sup>14</sup>V. V. Paranjape, Phys. Rev. B **52**, 10 740 (1995).

<sup>15</sup>G. Yong, Y. C. Li, X. J. Kong, and C. W. Wei, Phys. Rev. B **50**, 17 249 (1994).